References

[1]Hunter, L. W., and Kuttler, J. R., "The Enthalpy Method for Heat Conduction Problems with Moving Boundaries," *Journal of Heat Transfer*, Vol. 111, May 1989, pp. 239–242.

[2]Landau, H. G., "Heat Conduction in a Melting Solid," *Quarterly Applied Math*, Vol. 8, 1950, pp. 81–94.

[3]Kirchhoff, G., *Vorlesungen über die Theorie der warme,* Barth, Leipzig, Germany, 1984.

[4]Crank, J., and Nicolson, P., "A Practical Method of Numerical Evaluation of Solutions of Partial Differential Equations of the Heat Conduction Type," *Proceedings of the Cambridge Philosophical Society*, Vol. 43, 1947, pp. 50–67.

[5]Forsythe, G. E., and Wasow, W. R., *Finite-Difference Methods for Partial Differential Equations*, Wiley, New York, 1960, Chap. 2.

[6]Dongarra, J. J., Bunch, J. R., Moler, C. B., and Stewart, G. W., *Linpack User's Guide*, SIAM, Philadelphia, 1979.

[7]Randall, J. D., "Numerical Solution of the Embedding Equations Applied to the Landau Melting Problem," *International Journal of Heat and Mass Transfer*, Vol. 21, 1978, pp. 1447–1449.

Modification of COMMIX-1B for Simulation of Thermal- and Flowfields in Ultrahigh Temperature Vapor Core Reactor

James G. Zhang* and Samim Anghaie†
University of Florida,
Gainesville, Florida 32611

Introduction

THIS paper summarizes results of the COMMIX-1B computer code modification and numerical simulation of thermal- and flowfields in the closed-cycle Ultrahigh Temperature Vapor Core Reactor (UTVR) and magnetohydrodynamic (MHD) generator system. The UTVR-MHD system utilizes superheated uranium fluoride vapor nuclear fuel and an alkali metal such as potassium fluoride as the working fluid. The energy generation process and its conversion to electricity requires the flow of superheated fuel/working fluid at an average temperature in the range of 3000–5000 K through a fairly complex geometrical path. The nuclear kinetics behavior of this system is a strong function of both temperature and density of the vapor fuel/working fluid, which in turn has direct impact on power generation and heat release rate. This strong coupling among flow, heat transfer, and energy generation requires a careful modeling of these phenomena in the UTVR-MHD system. For analysis of the thermal hydraulics behavior of the high-power density fissioning gas in the reactor core, the COMMIX-1B[3] computer code has been modified to include a thermal and transport property package for uranium fluoride as well as a grid generation code and a plotting output display system.[1] Several power densities have been considered, and simulation results are presented.

Figure 1 shows the schematic of the geometry of a typical biomodal UTVR system with a disk MHD generator, which is used for simulation of the ultrahigh temperature vapor core reactor. The central cavity is designed to generate hundreds of megawatts in the burst mode. The mixture of uranium fluoride and working fluid comes to a nuclear critical condition in the reactor core. Flow of the fissioning vapor is treated as viscous, turbulent, compressible flow with variable thermodynamics and transport properties. The disk MHD generator and its associated converging-diverging nozzle convert the central cavity's energy to electricity at the average temperature of up to 5000 K. Heat transfer through the reactor wall can be very large, however, due to intensive cooling, the inner wall can be kept at a constant temperature in the range of 1500–2000 K. The fissioning gas flow rate in a UTVR can be controlled by adjusting the inlet and exit pressure difference provided that chocking conditions have not been reached at the nozzle throat surface. For the axisymmetric geometry of a UTVR vessel and the disk generator, the numerical model can be simplified to a two-dimensional, axisymmetric one.

Governing Equations

The flow of the uranium fluoride and the working fluid mixture through the UTVR-MHD system is modeled as viscous, turbulent, compressible flow with variable thermodynamics and transport properties. The computational model is designed to solve the unsteady, axisymmetric, partial differential equations for conservation of mass, momentum, and energy along with two equation (κ-ϵ) turbulence model. The system of governing equations in cylindrical coordinates system can be written in the following form[3]:

$$\frac{\partial(\rho\phi)}{\partial t}+\frac{\partial(\rho u\phi)}{\partial x}+\frac{\partial(\rho v\phi)}{\partial y}+\frac{\partial(\rho w\phi)}{\partial z}=\frac{\partial}{\partial x}\left(\Gamma_\phi\frac{\partial\phi}{\partial x}\right)+\frac{\partial}{\partial y}\left(\Gamma_\phi\frac{\partial\phi}{\partial y}\right)+\frac{\partial}{\partial z}\left(\Gamma_\phi\frac{\partial\phi}{\partial z}\right)+S_\phi \quad (1)$$

In this generalized governing equation, ϕ represents any of the dependent variables, Γ_ϕ is the diffusion coefficient, and S_ϕ represents the source term. A more detailed explanation of different terms in Eq. (1) is given in Ref. 3. All parameters in Eq. (1) are considered the time average value for turbulent flow, and the coefficient Γ_ϕ includes the turbulent diffusion terms.

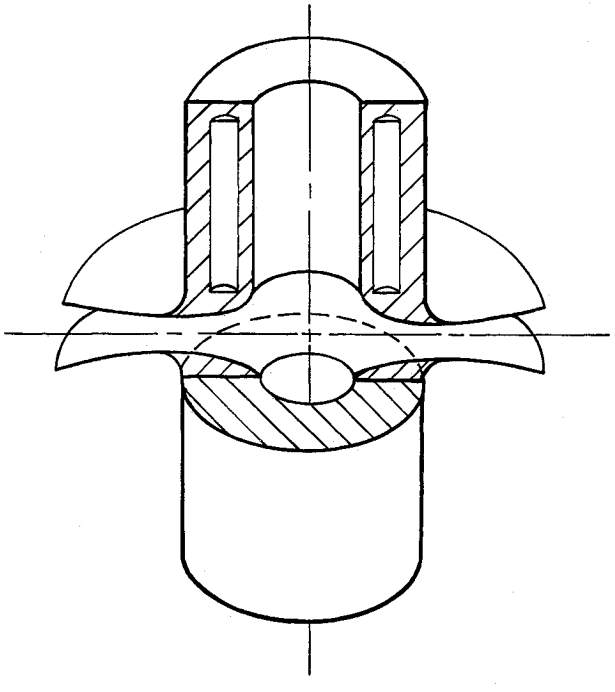

Fig. 1 Bimodal ultrahigh temperature vapor core reactor.

Presented as Paper 89-1990 at the AIAA 9th Computational Fluid Dynamics Conference, Buffalo, NY, June 13-15, 1989; received April 10, 1989; revision received Oct. 16, 1989.

*Postdoctoral Fellow, Innovative Nuclear Space Power Institude. Member AIAA.

†Associate Professor, Department of Nuclear Engineering Sciences.

Table 1 Coefficients of correlations given in Eqs. (4) and (5)

Temperature	a	b	c	d
$0<T<500$	4.43	4.05	2.57	8.96
$500<T<1000$	4.78	4.05	2.37	7.11
$1000<T<2000$	3.51	0.173	1.71	0.754

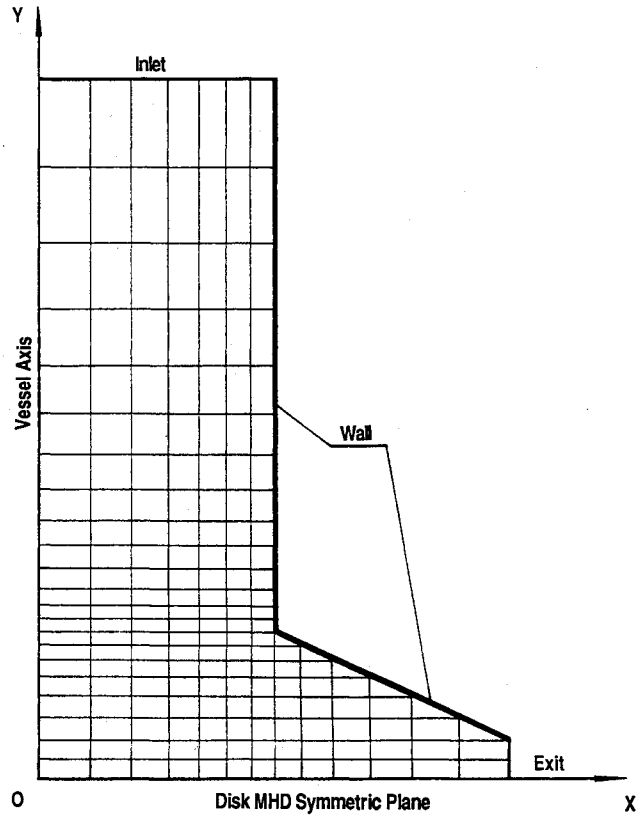

Fig. 2 Numerical model of UTVR-MHD.

Thermal and Transport Property Package

The prime candidates for fuel and working fluid in UTVR-MHD systems are uranium tetrafluoride (UF_4) and potassium fluoride (KF), respectively. At the present time, accurate information on the gaseous phase properties of these materials at high temperatures are not available. There is an ongoing effort by the authors to measure these properties at temperatures above 1500 K. For the purpose of the current code development and simulation effort, properties of uranium hexafluoride (UF_6) are used. The following experimental-based correlations provide UF_6 properties at temperatures up to 2000 K.

$$c_p = 0.448 + 1.86 \times 10^{-6} T - \frac{7.71 \times 10^3}{T^2} \tag{2}$$

$$\rho = \frac{1 + 1.2328 \times 10^6 \times P}{RT} \tag{3}$$

$$\mu = a \times 10^{-8} T + b \times 10^{-6} \tag{4}$$

$$\kappa = c \times 10^{-5} T + d \times 10^{-4} \tag{5}$$

where c_p is the specific heat, ρ is the density, μ is the viscosity, κ is the thermal conductivity, and P and T are the local pressure and temperature, respectively. Coefficients of Eqs. (4) and (5) are given in Table 1, and the SI unit is consistently used.

For temperatures above 2000 K, no reliable experimental data on properties of uranium hexafluorides are available yet. The perfect gas law is used to estimate the properties of uranium hexafluoride in the temperature range of 2000–5000 K.

Grid Generation

COMMIX-1B solves the Navier-Stokes equations in the physical domain using a skewed, upwind, finite-volume approach in a computational cell structure, which allows for one irregular surface. Supplying the necessary information on the model geometry for initiating the computational run with the standard version of COMMIX-1B is a slow and inefficient process. A grid-generation code is developed to prepare a regular computational mesh for calculation with the modified COMMIX-1B code. The grid-generation code is designed to determine the exact location of the irregular nodal points which fit the curved boundary. It also calculates the irregular cell surfaces and the normal unit vectors. The code is also designed to provide for small skewness, smoothness, and high resolution in the large gradient regions of the computational domain. These features are identified as the minimum required characteristics for a proper numerical grid-generation code.[5] To simulate the thermal- and flowfields in a UTVR-MHD system, the emphasis should be put on the high-resolution capability near the boundary of the reactor core and its radial nozzle where large gradients are expected. The numerical modeling is based on the grid system in Figs. 2 and 3.

An exponential clustering technique or a polynomial distribution function can be used to disperse the nonuniform grid along x- and y-axes.[4] Both methods are algebraic schemes, which cluster grid lines at the desired region within the domain or along the boundary. An exponential clustering function similar to the one given below provides the increment of interval between each pair of points along an arbitrary known curve, which can be determined by either an analytic function or coordinates of a few known points

$$\Delta S_k = \Delta S_0 (1 + \epsilon)^{k-1} \qquad k = 1, \ldots, k\max \tag{6}$$

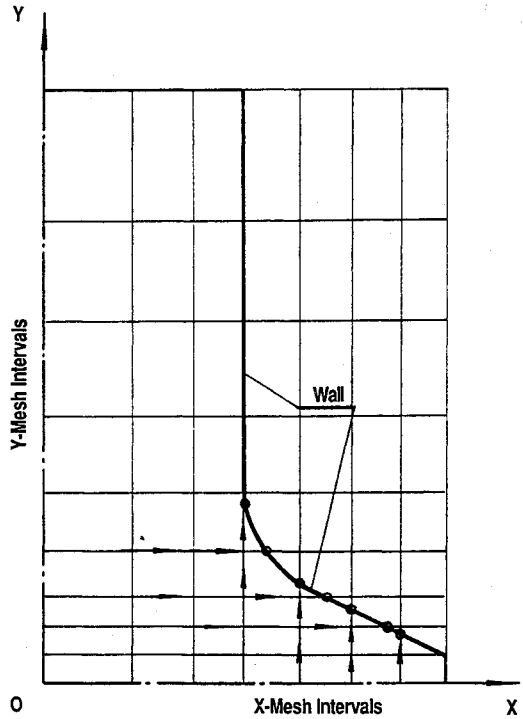

Fig. 3 Using dual-line shooting method to locate the nodal points along the irregular boundary.

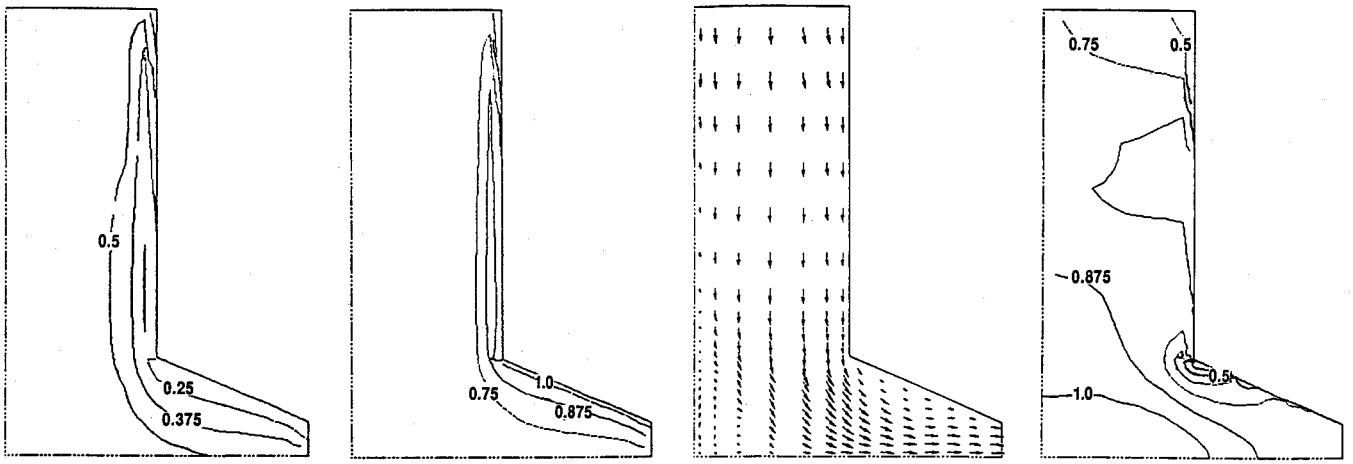

a) Temperature contour b) Density contour c) Flow pattern d) Pressure contour

Fig. 4 Temperature, density, and pressure contours and flow pattern in UTVR (P_{in} = 2 atm, UF_6 as working fluid).

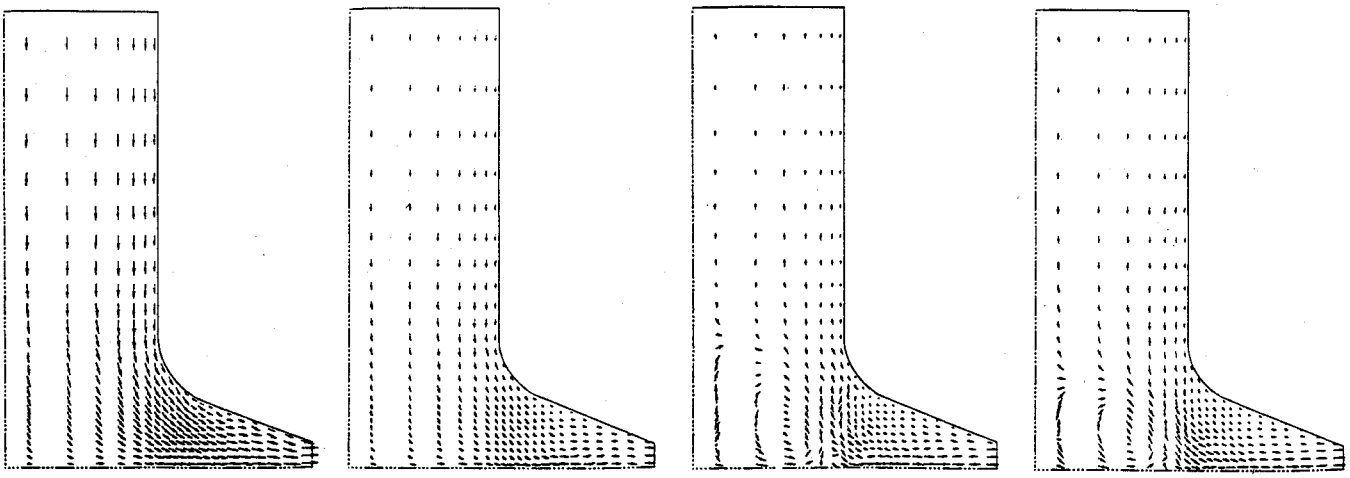

a) $Q = 1000$ W/m^3 b) $Q = 5000$ W/m^3 c) $Q = 10{,}000$ W/m^3 d) $Q = 20{,}000$ W/m^3

Fig. 5 Flow pattern of UF_6 gas in UTVR-MHD with different level heat sources Q (P_{in} = 20 atm, T_w = 1000 K, T_{in} = 1500 K).

In this equation, ΔS_0 is the minimum specified grid spacing next to the wall or to some inner boundaries in the vapor core reactor and $k$max is the maximum number of the points to be distributed along the curve. The parameter ϵ can be determined by a Newton-Raphson iteration process so that the sum of the above increments matches the known arc length of the curve. Once these increments are determined, the lengths of the clustered points along the given curve are computed, and the corresponding x and y coordinates can be determined using a cubic spline function or other interpolation methods. Contrary to the exponential technique, the polynomial distribution function directly redistributes one of the nodal point coordinates, say $X(X_0 < X_j < X_f)$, along a given curve by

$$X_j = X_0 + a\phi_j + b\phi_j^2 + c\phi_j^3 \tag{7}$$

where $\phi = (j - j_0)/(j_f - j_0)$, and j is the index value such that point j_0 to j_f lie in the interval X_0 to X_f, where $X_0 = X(j_0)$, $X_f = X(j_f)$ are x coordinates of the beginning and ending point of the segment, respectively. The coefficients a, b, c in Eq. (7) are given as

$$c = \frac{[\Delta X_f + \Delta X_0 - 2h(X_f - X_0)]}{(h - 3h^2 + 2h^3)}$$

$$b = \frac{[\Delta X_0 - h(X_f - X_0) - c(h^3 - h)]}{(h^2 - h)}$$

$$a = X_f - X_0 - b - c$$

where $h = 1/(j_f - j_0)$, and ΔX_0 and ΔX_f are the user-specified grid intervals at each end to control the degree of the clustering. The user can adjust these parameters to get satisfying distribution of grid points along a given curve. Similar to the exponential clustering function case, one may then use an interpolation function to find the other coordinate (in this case, y) at each node. Both grid-generation schemes are available in the modified COMMIX-1B code. For the simulation purposes that are presented in this paper, the exponential-clustering technique is used for generation of fine computational nodes in the direction of the reactor core axis; polynomial distribution functions are used for the direction of generation computational nodes in the direction of the nozzle-MHD axis.

To locate the irregular nodal points along the curved boundary, a dual-shooting, grid-lines technique is used. Using this technique, the possibility of crossing irregular cell surfaces can be prevented (Fig. 3). The major benefit in using such a clustered-cells system is the gain in resolution with which physical quantities can be calculated. It is also useful in preparation of input data for initiation of the computation with the modified COMMIX-1B code. These advantages are even more evident for systems with complex geometry and/or internal thermal structures where the fine clustered cells are always required.

Results and Discussion

As the first case, the flow of the fissioning UF_6 gas through a cylindrical reactor core and its radial nozzle is simulated. It

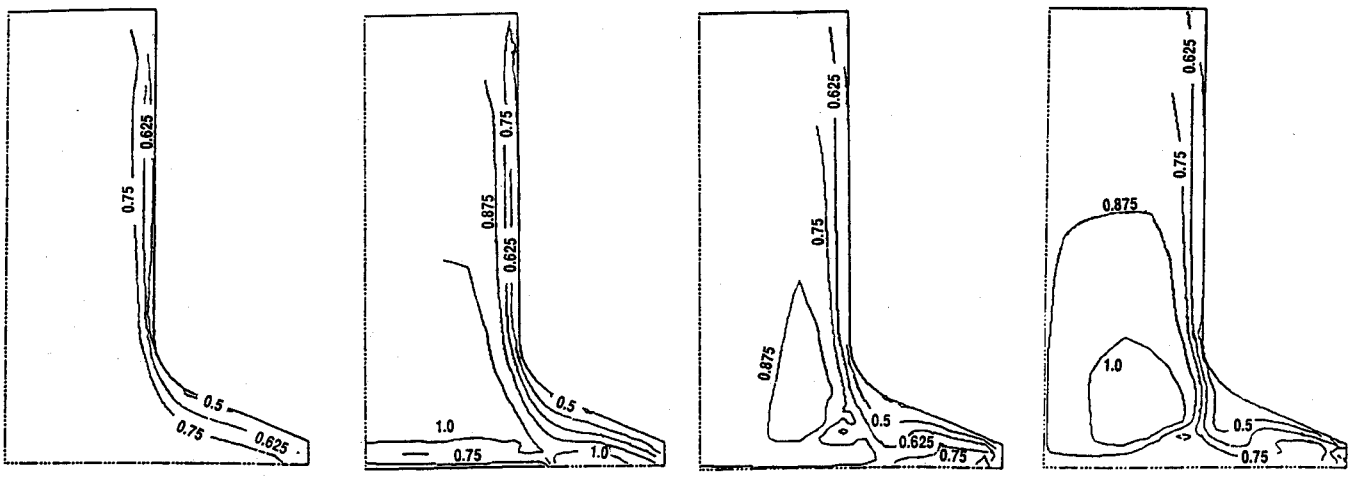

a) $Q = 1000$ W/m^3 b) $Q = 5000$ W/m^3 c) $Q = 10{,}000$ W/m^3 d) $Q = 20{,}000$ W/m^3

Fig. 6 Temperature contours of UF_6 gas flow in UTVR-MHD with different level heat sources Q($P_{in} = 20$ atm, $T_w = 1000$ K, $T_{in} = 1500$ K).

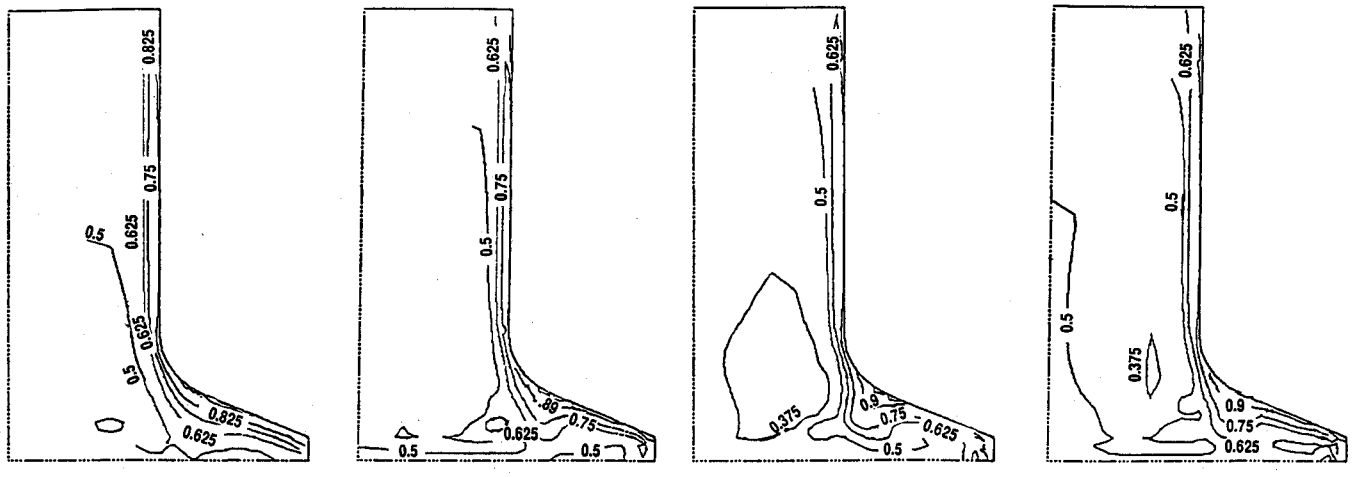

a) $Q = 1000$ W/m^3 b) $Q = 5000$ W/m^3 c) $Q = 10{,}000$ W/m^3 d) $Q = 20{,}000$ W/m^3

Fig. 7 Density contours of UF_6 gas flow in UTVR-MHD with different level heat sources Q($P_{in} = 20$ atm, $T_w = 1000$ K, $T_{in} = 1500$ K).

is assumed that the inlet pressure is 2 atm, the inlet temperature is 2000 K, and the wall temperature is maintained at 500 K. Figure 4 shows the computed flow pattern and the normalized temperature, density, and pressure contours in UTVR. It can be clearly seen that the density near the wall is much greater than that of the reactor core centerline. This is mainly due to the fact that the wall is kept at a temperature much less than the radial average temperature. In general the flow for this simulated case shows a laminar pattern.

In the second example case, simulation of thermal- and flowfields in UTVR-MHD with internal heat generation is considered. Arbitrary values of inlet parameters in the computed sample case of flow of the fissioning gas through the main reactor vessel were chosen for the code testing and for demonstration purposes. The inlet temperature is kept at 1500 K, and the temperature at the conducting wall surface is fixed at 1000 K. The inlet pressure is 20 atm, and the back pressure is fixed at 1 atm. The computed flow patterns and the normalized temperature and density contours of the superheated UF_6 vapor flow with a uniformly distributed heat source of 1000, 5000, 10,000, and 20,000 W/m^3 are shown in Figs. 5–7, respectively. The flowfield shows a very distinctive turbulent pattern as the internal heat source becomes larger. Higher temperatures occur at the central region of the UTVR core due to the existence of the heat sources and turbulence, whereas higher densities appear near the conducting wall where relative lower temperatures exist.

Concluding Remarks

The COMMIX-1B computer code has been modified and used for design analysis and simulation of thermal- and flowfields in the UTVR core. The major modification to this code includes development of a thermal and transport property package for uranium fluoride, a grid generation code, and a plotting output display system. The modified COMMIX-1B code is used as a preliminary computational tool for prediction of the thermofluid engineering features of the ultrahigh temperature vapor core reactor and its associated radial converging-diverging nozzle and disk MHD generator. The numerical, grid-generation code is designed to improve the solution efficiency and the accuracy of the calculation with COMMIX-1B. The plotting program provides a convenient way of presenting the computed results using the modified COMMIX-1B code. Numerical simulations of the thermal- and flowfields in the UTVR-MHD at a variety of the internal heat generation rates are performed.

Acknowledgments

This work presented here was funded by a grant from the Strategic Defense Initiative Organization, Division of Technology, Innovative Science under Contract F33615-88-C-2881 with the Wright-Patterson Air Force Base, through the Innovative Nuclear Space Power Institute.

References

[1]Anghaie, S., and Zhang, J. G., "Thermal Hydraulics," INSPI-FR-UF-88-002, Final Report, Vol. 2, Sec. 1.0, Dec. 1988.

[2]Dugan, E. T., Jacobs, A. M., Oliver, C. C., and Lear, W. E., Jr., "Acoustical Gas Core Reactor with MHD Power Generation for Burst Power in Bimodal System," *Transactions of the Fourth Symposia on Space Nuclear Power System*, Albuquerque, NM, Jan. 1987, pp. 149-152.

[3]Shah, V. L., "COMMIX-1B: A Three Dimensional Transient Single-Phase Computer Program for Thermal Hydraulic Analysis of Single and Multicomponent System," *Equations and Numerics,* Vol. 1, U.S. Government Printing Office, Washington DC, Sept. 1985, pp. 10-13.

[4]Steger, J. L., Nietubicz, C. Z., Hervey, K. R., "A General Curvilinear Grid Generations Problem for Projectile Configurations," U.S. Army BRL, Aberdeen Proving Ground, MD, Memorandum Rept. ARBRL-MR-03142, 1981.

[5]Thompson, J. F., Warsi, Z. U. A., and Mastin, C. W., "Boundary Fitted Coordinate System for Numerical Solution of Partial Differential Equations—A Review," *Journal of Computational Physics,* Vol. 47, July 1982, pp. 1-108.

Thermal Conductance of Two Space Station Cold Plate Attachment Techniques

G. P. Peterson,* G. Starks,† and L. S. Fletcher‡
Texas A&M University, College Station, Texas 77843

Introduction

TWO attachment techniques for mounting electronic equipment to space station cold plates were evaluated and compared. The characteristics investigated include the temperature variations and the thermal contact conductance at the electronic equipment/cold plate interface. Numerous investigations of heat transfer at the interface of two contacting metallic surfaces have been conducted including investigations dealing with the extent to which the thermal contact conductance can be improved using greases,[1] thin metallic foils,[2] or vapor deposited coatings.[3,4] Several excellent reviews which summarize these results and the other recent literature have been published.[5,6] In addition to these fundamental reviews, the results of several investigations directed specifically at the thermal contact conductance between components bolted onto single-phase liquid cold plates have been presented.[7-9]

The two techniques evaluated in this investigation included the standard 500 × 750 mm bolted cold plate, which utilizes 77 5-mm-diam bolts, approximately 15 mm in length and spaced on a 70 × 70 mm matrix pattern as shown in Fig. 1, and a flexible pressurized bladder. In normal operation, the pressurized bladder would be placed behind the devices to be cooled, clamping the base plate of the devices to the cold plate and eliminating the need for bolts.

In order to determine the effectiveness and thermal characteristics of these two attachment techniques, an experimental investigation was conducted using a specially developed thermal test plate and a flight-ready cold plate provided by Marshall Space Flight Center. Measurements of the surface temperature variation and the thermal contact conductance at the interface of the test plate and the cold plate were made for both attachment techniques.

For the purpose of this investigation, the heat source was simulated by an electrically heated, 500 × 750 mm aluminum 6061-T6 plate 2.54 cm thick. A series of 77 5-mm bolt holes 12.7 mm deep were drilled and tapped in the aluminum plate on 70-mm centers to match the bolt matrix of the cold plate. After tapping the bold holes, the aluminum plate was machined and ground to an overall flatness deviation of 0.1 mm with an rms surface roughness of 0.0032 mm.

Four silicone rubber resistance heaters, each with a rated capacity of 2250 W, were installed on the backside of the thermal test plate with silicone adhesive. The power to each heater was measured by both a digital Wattmeter and a multimeter used to measure the voltage and current. The temperature of the cold plate was controlled by varying the temperature of water flowing through a constant temperature circulating bath at a flow rate of 0.13 kg/s (2 gal/min).

In order to determine the thermal contact conductance and temperature variation at the contacting surface, the regions around four different bolt holes were instrumented. Around each hole, a series of 1.2-mm-diam thermocouple wells were drilled from the backside of the thermal test plate at four different radii, as illustrated in Fig. 1. A Chromel-Alumel thermocouple (AWG-36) was inserted and packed into each thermocouple well with a thermally conductive epoxy. Small channels were machined on the backside of the thermal test plate for the thermocouple wires and sealed with epoxy. In addition to a three-dimensional temperature profile around each bolt, this combination of thermocouples provided a means by which the thermal test plate surface temperature could be obtained at each radial distance.

The inflatable bladder used in this investigation (constructed by ILC Dover of Frederica, Delaware) was proof tested to 0.2071 MPa (30 psi) but was only operated to a pressure of 0.138 MPa (20 psi). The bladder was equipped with a standard Schrader valve. Pressure in the bladder was

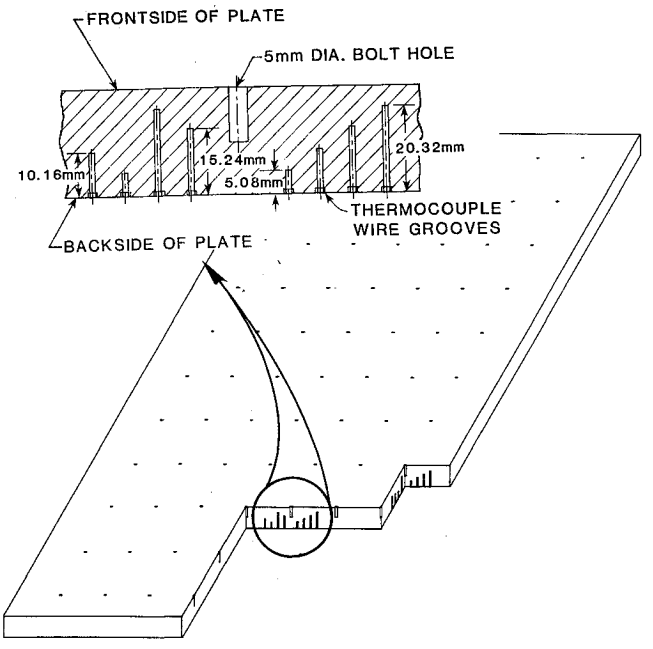

Fig. 1 Thermal test plate and thermocouple well locations.

Received June 8, 1989; presented as Paper 89-1703 at the AIAA 24th Thermophysics Conference, Buffalo, NY, June 12-14, 1989; revision received Aug. 29, 1989.

*Associate Professor, Department of Mechanical Engineering. Member AIAA.

†Graduate Research Assistant, Department of Mechanical Engineering.

‡Dietz Professor, Department of Mechanical Engineering. Fellow AIAA.